

Synthesis and Light Emitting Properties of Polyacetylenes Having Pendent Fluorene Groups

CHUN-HAO HUANG, SHENG-HSIUNG YANG, KUEI-BAI CHEN, CHAIN-SHU HSU

Department of Applied Chemistry, National Chiao Tung University, Hsinchu 30010, Taiwan, Republic of China

Received 11 August 2005; accepted 29 September 2005

DOI: 10.1002/pola.21163

Published online in Wiley InterScience (www.interscience.wiley.com).

ABSTRACT: Five novel fluorene-containing polymers, poly[(9,9-dimethylfluorene-2-yl)acetylene] (**PFA1**), poly[(1-pentyl-2-(9,9-dimethylfluorene-2-yl)acetylene] (**PFA2**), poly[1-decyl-2-(9,9-dimethylfluorene-2-yl)acetylene] (**PFA3**), poly[1-phenyl-2-(9,9-dimethylfluorene-2-yl)acetylene] (**PFA4**), and poly[1-(3,4-difluorophenyl)-2-(9,9-dimethylfluorene-2-yl)acetylene] (**PFA5**) were synthesized by the polymerization of the corresponding fluorene-substituted acetylenic monomers (**M1–M5**), using WCl_6 , $MoCl_5$, and $TaCl_5$ as catalysts and $n-Bu_4Sn$ as a cocatalyst. The synthesized polymers were thermally stable and readily soluble in common organic solvents. The degradation temperatures for a 5% weight loss of the polymers were ~ 352 – 503 °C under nitrogen. **PFA1–PFA5** show emission peaks from 402 to 590 nm. Besides, their electroluminescent properties were studied in heterostructure light-emitting diodes (LEDs), using **PFA2–PFA5** as an emitting layer. The **PFA5** device revealed an orange-red emission peak at 602 nm with a maximum luminescence of 923 cd/m^2 at 8 V. A device with the ITO/PEDOT/ a mixture of **PFA2** (98 wt %) and **PFA5** (2 wt %)/Ca/Al showed near white emission. Its maximum luminance and current efficiency are 450 cd/m^2 at 15 V and 1.3 cd/A, respectively. © 2005 Wiley Periodicals, Inc. *J Polym Sci Part A: Polym Chem* 44: 519–531, 2006

Keywords: fluorescence; light-emitting diodes (LED); photoluminescence; polyacetylene

INTRODUCTION

Conjugated polymers have been extensively studied for their potential applications in light emitting diodes,¹ organic lasers,² thin film transistors,³ and solar cells.⁴ Polyacetylene is a prototypical conjugated polymer among many promising conjugated polymers, which exhibits high conductivity upon doping.⁵ The conductivities of this polymer can reach as high as 10^5 S/cm .⁶ Although polyacetylene shows a very high electrical conductivity by doping, this polymer has rarely been used as a light-emitting polymer for electroluminescent (EL) devices because nonsubstituted polyacetylene is

insoluble, infusible, and unstable in air and exhibits almost no photoluminescence (PL) in the visible region.

Substituted polyacetylenes such as poly(phenylacetylene) (PPA) were reported by Percec and coworkers.^{7–10} Recently, Masuda and coworkers,^{11–15} Tang and coworkers,^{16–19} and our laboratory²⁰ have also synthesized several series of disubstituted polyacetylene derivatives, which were stable in air and soluble in common organic solvents. Although the conductivities of these polyacetylene derivatives are not as high as those of nonsubstituted ones, some show both PL and EL properties in the visible wavelength region. The most commonly used substituents for these polyacetylene derivatives are the alkyl and phenyl groups. These alkyl or phenyl-substituted polyacetylenes can emit red to blue light based on different substituents. In general, the PL efficien-

Correspondence to: C. S. Hsu (E-mail: cshsu@mail.nctu.edu.tw)

Journal of Polymer Science: Part A: Polymer Chemistry, Vol. 44, 519–531 (2006)
© 2005 Wiley Periodicals, Inc.

cies of disubstituted polyacetylenes are higher than those of monosubstituted polyacetylenes.²¹ The EL efficiencies of these substituted polyacetylenes are rather low. The best EL device using poly[1-(*p*-butylphenyl)-2-phenylacetylene] doped with 2-(4-biphenyl)-5-(4-*t*-butylphenyl)-1,3,4-oxadiazole as emitting materials was reported.¹¹ Its quantum yield, current efficiency, and luminescence were 0.1%, 0.038 cd/A, and 30 cd/m², respectively.

Recently, a naphthalene, a silole, or a carbazole pendant was incorporated into a poly(1-phenyl-1-alkyne) structure by Tang and coworkers.^{16–18} They found that the materials not only exhibited a higher thermal stability, but also emitted a strong blue light. They showed much higher quantum efficiencies than those of alkyl- and phenyl-substituted polyacetylenes. For example, an EL device¹⁷ with the configuration of ITO/poly[1-phenyl-5-(α -naphthoxy)pentyne]: PVK/bathocuproine/Alq3/LiF/Al, emitted blue light of 468 nm with a maximum brightness of 955 cd/m² and a power efficiency of 0.18 lm/W. Sanda et al.¹⁵ also reported some polyacetylenes with pendant carbazole groups. The EL devices based on poly(3,6-ditertbutyl-*N*-(*p*-ethynylphenyl)carbazole) in conjunction with iridium complexes exhibited brightness from 13 to 18 cd/m².

The polymers containing fluorene moieties in the main chain or side-chain have attracted considerable attention because of their unique properties of EL applications.^{22–28} Recent examples of the polymers containing pendant fluorene moieties include poly(vinylfluorene),²⁵ poly(fluorenylacetylene),²⁶ and poly(fluorenylphenylene vinylene).^{27,28} The bulky fluorene pendant also affects the polymer packing and reduces chain interaction between the polymer backbones. This will improve the performance of polymer light emitting diodes (PLED). In this paper, we incorporated a fluorene unit into the polyacetylene backbones, and investigated their peculiar PL and EL properties.

EXPERIMENTAL

Materials

Bis(triphenylphosphine)palladium(II) chloride (PdCl₂(PPh₃)₂, 99.99%), copper(I) iodide (CuI, 98%), triphenylphosphine (PPh₃, 99%), 2-methyl-3-butyn-2-ol (98%), tetra-*n*-butyltin (*n*-Bu₄Sn), molybdenum(V) chloride (MoCl₅, 99.9%), and tan-

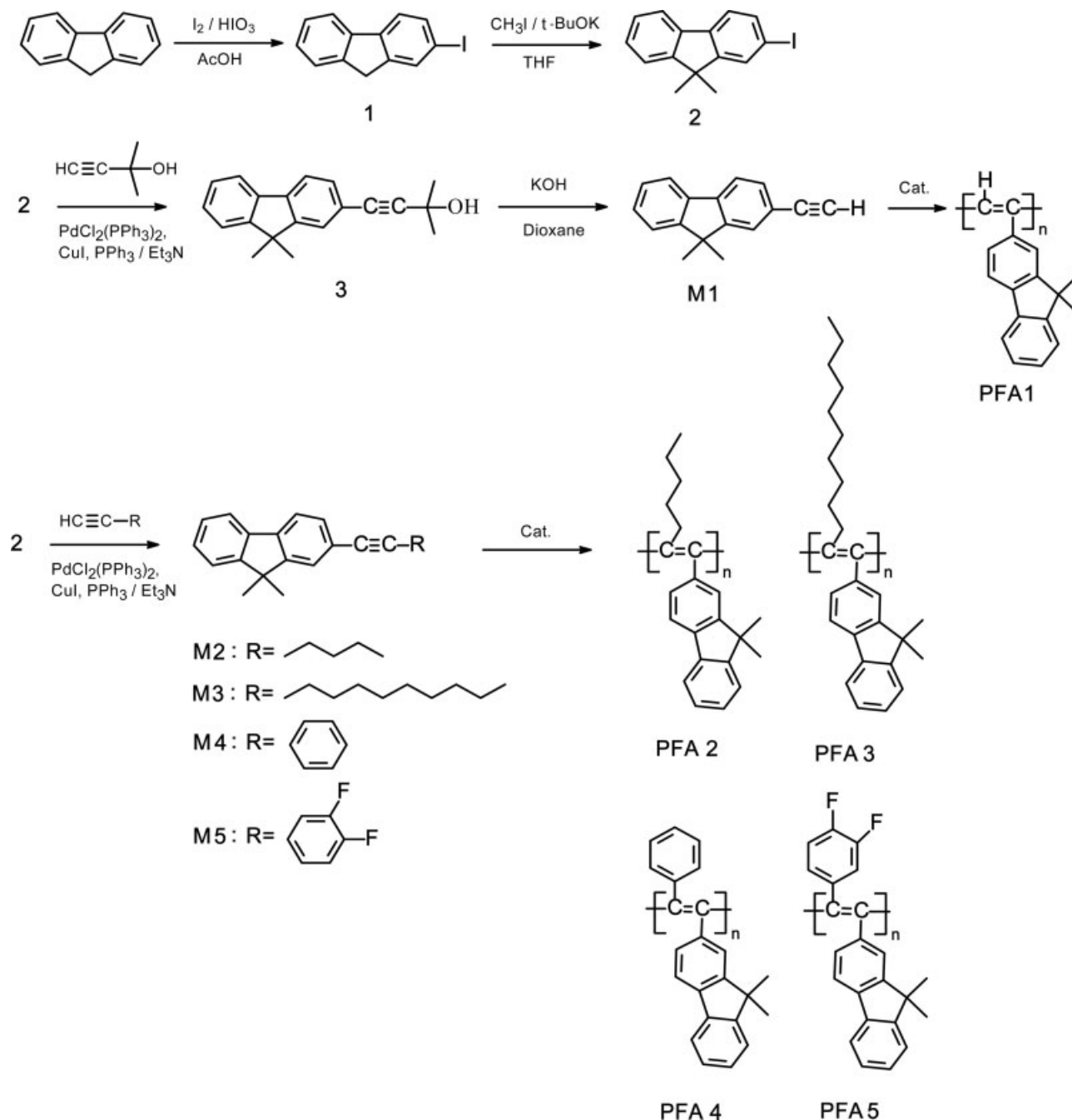
talum(V) chloride (TaCl₅, 99.99%) were purchased from Aldrich. Tungsten(VI) chloride (WCl₆) was purchased from ACROS. All commercial products were used without further purification. Tetrahydrofuran (THF) was dried over sodium, and dioxane, triethylamine (Et₃N), and *N,N*-dimethylformamide (DMF) were dried over calcium hydride and then distilled under nitrogen.

Techniques

¹H and ¹³C NMR spectra (300 MHz) were recorded on a Varian VXR-300 spectrometer. Fourier transform infrared (FTIR) spectra were recorded as KBr pellets on Perkin Elmer Spectra 1 spectrometer. Mass spectra were obtained on a JEOL JMS-SX 102A mass spectrometer. Thermal transitions and thermodynamic parameters were determined by using a Perkin Elmer Pyris 1 differential scanning calorimeter equipped with a liquid-nitrogen cooling accessory. Heating and cooling rates were 10 °C/min. Gel permeation chromatography (GPC) was run on a Waters 510 LC instrument equipped with a 410 differential refractometer, a UV detector, and a set of polystyrene gel columns of 10², 5 × 10², 10³, and 10⁴ Å. The oven temperature was set at 40 °C. THF was used as eluent and the flow rate was 1 mL/min. The UV–visible spectra and photoluminescence spectra of polymers were measured from an HP 8453 diode-array spectrophotometer and a Hitachi F-4500 luminescence spectrophotometer, respectively. The PL quantum yield (ϕ_f) in chloroform solution was measured by integrated sphere. Meanwhile, cyclic voltammetric (CV) measurements were made in acetonitrile (CH₃CN) with 0.1 M tetrabutylammonium hexafluorophosphate (TBAPF₆) as the supporting electrolyte at a scan rate of 50 mV/s. Platinum wires were used as both the counter and working electrodes, and silver/silver ions (Ag in 0.1 M AgNO₃ solution, from Bioanalytical Systems, Inc.) were used as the reference electrode. The PLED characterization was carried out by a Keithley 2400 source-measure unit and a calibrated silicon photodiode. The brightness was further measured using a Photo Research PR650 spectrophotometer.

Synthesis of Monomers M1–M5

The synthesis of fluorine-substituted acetylenic monomers **M1–M5** is outlined in Scheme 1.



Scheme 1. Synthesis of monomers M1–M5 and polymers PFA1–PFA5.

2-Iodofluorene (1)

Fluorene (30.0 g, 180 mmol), iodine (23.0 g, 91 mmol), and iodic acid (HIO_3) (8.0 g, 45 mmol) were dissolved in 80% acetic acid aqueous solution containing a small amount of sulfuric acid. The reaction mixture was heated at 80 °C for 4 h under nitrogen atmosphere. After the solution was cooled, the solvent was removed by decanta-

tion. The product was washed with methanol and dried to yield 31.6 g (60%) of brown solid; mp: 130–132 °C.

^1H NMR (300 MHz, CDCl_3) δ (ppm): 3.81 (d, $J = 15.9$ Hz, 2H), 7.31 (m, 2H), 7.44 (m, 2H), 7.66 (d, $J = 7.2$ Hz, 1H), 7.73 (d, $J = 7.2$ Hz, 1H), 7.85 (s, 1H). ^{13}C NMR (75 MHz, CDCl_3) δ (ppm): 36.6, 92.5, 120.2, 121.7, 122.3, 127.1, 127.8, 132.2,

135.9, 138.0, 138.6, 153.2, 154.9. MS [M^+] calcd. for $C_{13}H_9I$ 292.12, found 292. ELEM. ANAL. Calcd. for $C_{13}H_9I$: C, 53.45; H, 3.11. Found: C, 53.40; H, 3.18.

9,9-Dimethyl-2-iodofluorene (2)

2-Iodofluorene (25.0 g, 85.6 mmol) was dissolved in THF and treated with potassium *tert*-butoxide (21.8 g, 0.19 mol) to give a red solution, followed by methylation with methyl iodide (28.2 g, 0.19 mol) at room temperature for 3 h. The product was purified by column chromatography (silica gel, *n*-hexane as eluent, and Rf 0.7) to yield 25.2 g (92%) of yellow solid; mp: 63–65 °C.

1H NMR (300 MHz, $CDCl_3$) δ (ppm): 1.47 (s, 6H), 7.31 (m, 2H), 7.44 (m, 2H), 7.66 (d, $J = 7.2$ Hz, 1H), 7.73 (d, $J = 7.2$ Hz, 1H), 7.85 (s, 1H). ^{13}C NMR (75 MHz, $CDCl_3$) δ (ppm): 26.9, 47.1, 92.5, 120.0, 121.7, 122.5, 127.1, 127.8, 132.0, 135.9, 138.0, 138.6, 153.0, 154.9. MS [M^+] calcd. for $C_{15}H_{13}I$ 320.17, found 320. ELEM. ANAL. Calcd. for $C_{15}H_{13}I$: C, 56.27; H, 4.09; I, 39.64. Found: C, 56.21; H, 4.12.

9,9-Dimethyl-2-(3-hydroxy-3-methyl-1-butynyl)-fluorene (3)

9,9-Dimethyl-2-iodofluorene (25.0 g, 78.1 mmol), $PdCl_2(PPh_3)_2$ (0.56 g, 0.78 mmol), CuI (1.53 g, 5.86 mmol), and PPh_3 (0.74 g, 3.9 mmol) were dissolved in Et_3N (250 mL), and the mixture was stirred under nitrogen. After all the catalysts were dissolved, 2-methyl-3-butyn-2-ol (7.88 g, 93.7 mmol) was added. The resulting solution was heated at 70 °C for 12 h. After Et_3N was removed under reduced pressure, the product was extracted with diethyl ether. The crude product was isolated by evaporating the solvent and purified by column chromatography (silica gel, ethyl acetate: *n*-hexane = 1:5 as eluent, and Rf 0.4) to yield 13.0 g (68%) of brown oil.

1H NMR (300 MHz, $CDCl_3$) δ (ppm): 1.47 (s, 6H), 1.65 (s, 6H), 7.31 (m, 2H), 7.41 (m, 2H), 7.48 (s, 1H), 7.66 (m, 2H). ^{13}C NMR (75 MHz, $CDCl_3$) δ (ppm): 26.9, 31.4, 46.8, 66.7, 81.2, 90.4, 119.8, 120.3, 122.5, 122.6, 126.4, 127.0, 127.8, 131.2, 138.2, 140.0, 153.9, 154.0. MS [M^+] calcd. for $C_{20}H_{20}O$ 276.38, found 276. ELEM. ANAL. Calcd. for $C_{20}H_{20}O$: C, 89.92; H, 7.29; O, 5.79. Found: C, 89.94; H, 7.23.

1-(9,9-Dimethylfluorene-2-yl)acetylene (M1)

9,9-Dimethyl-2-(3-hydroxy-3-methyl-1-butyl)-fluorene (10.0 g, 36 mmol) and KOH (4.44 g, 79.2 mmol) were dissolved in dioxane (300 mL). The mixture was heated at 120 °C for 4 h, cooled to room temperature, and 6 N HCl aqueous solution (12 mL) was added. The resulting solution was extracted with ethyl ether. The crude product was isolated by evaporating the solvent and purified by column chromatography (silica gel, *n*-hexane as eluent, Rf 0.55) to yield 5.8 g (74%) of colorless oil.

1H NMR (300 MHz, $CDCl_3$) δ (ppm): 1.47 (s, 6H), 3.12 (s, 1H), 7.32 (m, 2H), 7.44 (m, 2H), 7.56 (s, 1H), 7.64 (d, $J = 7.2$ Hz, 1H), 7.67 (d, $J = 7.2$ Hz, 1H). ^{13}C NMR (75 MHz, $CDCl_3$) δ (ppm): 26.9, 46.8, 77.0, 84.4, 119.8, 120.3, 122.5, 122.6, 126.4, 127.0, 127.8, 131.2, 138.2, 140.0, 153.9, 154.0. MS [M^+] calcd. for $C_{17}H_{14}$ 218.30, found 218. ELEM. ANAL. Calcd. for $C_{17}H_{14}$: C, 93.54; H, 6.46. Found: C, 93.53; H, 6.47.

1-Pentyl-2-(9,9-dimethylfluorene-2-yl)acetylene (M2), 1-Decyl-2-(9,9-dimethylfluorene-2-yl)acetylene (M3), 1-Phenyl-2-(9,9-dimethylfluorene-2-yl)acetylene (M4), and 1-(3,4-Difluorophenyl)-2-(9,9-dimethylfluorene-2-yl)acetylene (M5)

Monomers **M2–M5** were synthesized by a similar method. The preparation of monomer **M2** is described here. 9,9-Dimethyl-2-iodofluorene (10 g, 31.2 mmol), $PdCl_2(PPh_3)_2$ (0.22 g, 0.31 mmol), CuI (0.62 g, 2.37 mmol), and PPh_3 (0.24 g, 1.26 mmol) were dissolved in Et_3N (100 mL), and the mixture was stirred at room temperature under nitrogen. After all catalysts were dissolved, 1-heptyene (3.6 g, 37.5 mmol) was added. The resulting solution was reacted at 70 °C for 12 h. After Et_3N was removed under reduced pressure, the product was extracted with diethyl ether. The crude product was isolated by evaporating the solvent and purified by column chromatography (silica gel, *n*-hexane as eluent, and Rf 0.6) to yield 4.76 g (53%) of colorless oil.

1H NMR (300 MHz, $CDCl_3$) δ (ppm): 0.93 (t, 3H), 1.48 (m, 10H), 1.62 (m, 2H), 2.43 (t, 2H), 7.32 (m, 2H), 7.40 (m, 2H), 7.46 (s, 1H), 7.61 (d, $J = 7.2$ Hz, 1H), 7.63 (d, $J = 7.2$ Hz, 1H). ^{13}C NMR (75 MHz, $CDCl_3$) δ (ppm): 14.0, 19.4, 22.2, 26.9, 28.5, 31.1, 46.7, 81.2, 90.4, 119.7, 120.1, 122.5, 122.6, 125.8, 127.0, 127.3, 130.5, 138.5, 138.6, 153.4, 153.7. MS [M^+] calcd. for $C_{22}H_{24}$ 288.43,

found 288. ELEM. ANAL. Calcd. for $C_{22}H_{24}$: C, 91.61; H, 8.39. Found: C, 91.60; H, 8.40.

M3

Yield: 51%. 1H NMR (300 MHz, $CDCl_3$) δ (ppm): 0.9 (t, 3H), 1.27 (m, 13H), 1.46(m, 7H), 1.62 (m, 2H), 2.43 (t, 2H), 7.32 (m, 2H), 7.39 (m, 2H), 7.46 (s, 1H), 7.61 (d, $J = 7.2$ Hz, 1H), 7.64 (d, $J = 7.2$ Hz, 1H). ^{13}C NMR (75 MHz, $CDCl_3$) δ (ppm): 14.1, 19.4, 22.6, 26.9, 28.8, 29.0, 29.2, 29.3, 29.5, 29.6, 31.9, 46.7, 81.2, 90.4, 119.7, 120.1, 122.5, 122.6, 125.8, 127.0, 127.3, 130.5, 138.5, 138.6, 153.4, 153.7. MS [M^+] calcd. for $C_{27}H_{34}$ 358.57, found 358. ELEM. ANAL. Calcd. for $C_{27}H_{34}$: C, 90.44; H, 9.56. Found: C, 90.40; H, 9.60.

M4

Yield: 70%. mp: 112–114 °C. 1H NMR (300 MHz, $CDCl_3$) δ (ppm): 1.50 (s, 6H), 7.34 (m, 4H), 7.43 (m, 2H), 7.51 (m, 3H), 7.60 (s, 1H), 7.70 (d, $J = 7.8$ Hz, 2H). ^{13}C NMR (75 MHz, $CDCl_3$) δ (ppm): 26.9, 46.8, 89.5, 90.4, 119.9, 120.3, 121.9, 122.5, 122.6, 123.0, 126.0, 127.0, 127.1, 127.7, 128.1, 128.3, 130.7, 131.6, 138.2, 139.4, 153.9, 154.0. MS [M^+] calcd. for $C_{23}H_{18}$ 294.40, found 294. ELEM. ANAL. Calcd. for $C_{23}H_{18}$: C, 93.84; H, 6.16. Found: C, 93.74; H, 6.26.

M5

Yield: 67%. mp: 102–104 °C. 1H NMR (300 MHz, $CDCl_3$) δ (ppm): 1.50 (s, 6H), 7.14 (q, 1H), 7.35 (m, 3H), 7.49 (d, 1.5 Hz, 1H), 7.52 (d, 1.5 Hz, 1H), 7.58 (d, 1.5 Hz, 1H), 7.69 (s, 1H), 7.70 (m, 2H). ^{13}C NMR (75 MHz, $CDCl_3$) δ (ppm): 26.9, 46.8, 87.2, 90.3, 117.5 (d), 119.9, 120.3, 120.4 (d), 121.0, 122.5, 122.6, 126.0, 127.1, 127.8, 128.0 (d), 128.1 (d), 130.7, 138.2, 139.8, 148.2 (d), 148.5 (d), 151.9 (d), 152.2 (d), 153.6, 153.8. MS [M^+] calcd. for 330.38, found 330. ELEM. ANAL. Calcd. for $C_{23}H_{16}F_2$: C, 83.62; H, 4.88. Found: C, 83.60; H, 4.91.

Polymerization of Monomers M1–M5

Polymerizations were carried out under nitrogen using either an inert atmosphere glove box or a Schlenk tube in a vacuum line system, except for the purification of the polymers, which was done in an open atmosphere. An experimental procedure for the polymerization of monomer **M1** is given here.

Monomer **M1** (0.9 g, 4.12 mmol) was added into a Schlenk tube with a three-way stopcock on the sidearm. The tube was evacuated under vacuum and then flushed with nitrogen three times through sidearm. Toluene (10 mL) was injected into the tube through a septum to dissolve the monomer. The initiator solution was prepared in another tube by dissolving WCl_6 (0.158 g, 0.4 mmol) and $n-Bu_4Sn$ (0.28 mg, 0.8 mmol) in 10 mL of dried toluene. Both tubes were aged at room temperature for 30 min. The initiation solution was injected into the monomer solution, and the reaction mixture was stirred at 30 °C under N_2 for 24 h. The solution was then cooled to room temperature, diluted with 2 mL of THF and added drop-wise through a cotton filter to 300 mL of methanol with stirring. The polymer was separated by filtration, purified by several reprecipitations from THF into methanol, and dried in vacuum to yield 0.61 g (68%) of **PFA1**.

1H NMR (300 MHz, $CDCl_3$) δ (ppm): 1.48 (s, 6H), 7.19 (br, 3H), 7.23 (br, 3H), 7.64 (br, 2H). ^{13}C NMR (75 MHz, $CDCl_3$) δ (ppm): 26.9, 46.8, 119.8, 120.3, 122.5, 122.6, 126.4, 127.0, 127.8, 131.2, 138.2, 140.0, 153.9, 154.0, 155.0. ELEM. ANAL. Calcd. for $C_{17}H_{14}$: C, 93.54; H, 6.46. Found: C, 92.64; H, 6.46.

PFA2

Yield: 31%. 1H NMR (300 MHz, $CDCl_3$) δ (ppm): 0.93 (t, 3H), 1.47 (br, 12H), 2.18 (t, 2H), 7.17 (br, 5H), 7.62 (br, 2H). ^{13}C NMR (75 MHz, $CDCl_3$) δ (ppm): 14.0, 19.4, 26.9, 28.5, 31.1, 45.7, 119.7, 120.1, 122.5, 122.6, 125.8, 127.0, 127.3, 130.5, 138.5, 138.6, 140.0, 153.4, 153.7. ELEM. ANAL. Calcd. for $C_{22}H_{24}$: C, 91.64; H, 8.39. Found: C, 89.00; H, 8.10.

PFA3

Yield: 36%. 1H NMR (300 MHz, $CDCl_3$) δ (ppm): 0.93 (t, 3H), 1.27–1.55 (br, 22H), 2.20 (t, 2H), 7.32 (br, 5H), 7.6 (br, 2H). ^{13}C NMR (75 MHz, $CDCl_3$) δ (ppm): 14.1, 19.4, 22.6, 26.9, 28.8, 29.0, 29.2, 29.3, 29.5, 29.6, 31.9, 46.7, 119.7, 120.1, 122.5, 122.6, 125.8, 127.0, 127.3, 130.5, 138.5, 138.6, 146.5, 153.4, 153.7. ELEM. ANAL. Calcd. for $C_{27}H_{34}$: C, 90.44; H, 9.56. Found: C, 88.54; H, 9.40.

Table 1. Polymerization of Fluorene-Containing Monomers M1–M5^a

Monomer	Cat.	Temp. (°C)	Yield (%)	M_n^b	PDI	T_g (°C)	T_d (°C) ^c
M1	WCl ₆	30	68.2	40,500	1.88	76.4	372
M1	MoCl ₅	30	57.6	35,000	1.52	76.0	371
M2	TaCl ₅	80	30.9	7500	1.35	75.7	377
M3	TaCl ₅	80	36.0	8900	1.45	76.3	387
M4	TaCl ₅	80	75.3	315,700	3.12	81.5	462
M5	TaCl ₅	80	69.2	285,100	2.88	84.4	503

^a All polymerization took place under nitrogen for 24 h in toluene solution and used *n*-Bu₄Sn as cocatalyst. [M] = 0.2M, [WCl₆] = [MoCl₅] = [TaCl₅] = 20 mM, [*n*-Bu₄Sn] = 40 mM.

^b Determined by GPC relative to polystyrene.

^c Temperature of 5% weight loss measured by TGA in nitrogen.

PFA4

Yield: 75%. ¹H NMR (300 MHz, CDCl₃) δ (ppm): 1.58 (s, 6H), 7.40 (br, 6H), 7.55 (br, 4H), 7.70 (br, 2H). ¹³C NMR (75 MHz, CDCl₃) δ (ppm): 26.9, 46.8, 119.9, 120.3, 121.9, 122.5, 122.6, 123.0, 126.0, 127.0, 127.1, 127.7, 128.1, 128.3, 130.7, 131.6, 138.2, 139.4, 153.9, 153.0, 156.4. ELEM. ANAL. Calcd. for C₂₃H₁₈: C, 93.84; H, 6.16. Found: C, 92.20; H, 5.89.

PFA5

Yield: 70%. ¹H NMR (300 MHz, CDCl₃) δ (ppm): 1.58 (s, 6H), 7.15 (br, 1H), 7.35 (br, 3H), 7.50 (br, 3H), 7.68 (br, 3H). ¹³C NMR (75 MHz, CDCl₃) δ (ppm): 26.9, 46.8, 117.5 (d), 119.9, 120.3, 120.4 (d), 121.0, 122.5, 122.6, 126.0, 127.1, 127.8, 128.0 (d), 128.1 (d), 130.7, 138.2, 139.8, 148.2 (d), 148.5 (d), 151.9 (d), 152.2 (d), 153.6, 153.8, 156.2. ELEM. ANAL. Calcd. for C₂₃H₁₆F₂: C, 83.62; H, 4.88. Found: C, 82.66; H, 5.22.

Fabrication of EL Devices

The light-emitting devices were prepared on ITO-coated glass substrates, which were pre-cleaned and treated with UV ozone for 3 min before use. The poly(ethylene dioxythiophene):poly(styrene sulfonate) (PEDOT:PSS) was purchased from Bayer Co. The PEDOT layer was spin-coated with a spin rate of 6500 rpm onto the pretreated ITO substrates and cured at 200 °C for 10 min under vacuum. The emissive layer was then spin-coated on the top of the hole-transporting layer from a toluene solution of the polymer (0.6% in wt/v) with a spin rate of 1200 rpm. The thickness of the organic layer was measured on a Sloan Dektak 3030 surface profiler. The thickness of the PEDOT layer was about 40–50 nm, and the thickness of the polymer layer was about 80–100 nm. A layer of 35-nm thick calcium

(Ca) cathode was vacuum-deposited at a pressure of about 8×10^{-7} Torr. An additional protecting layer of 100-nm thick aluminum (Al) was then vacuum-evaporated on top of the Ca layer under the same condition.

RESULTS AND DISCUSSION

Polymer Synthesis

Table 1 summarizes the conditions and results of the polymerization of the fluorene-substituted acetylenic monomers, using WCl₆, MoCl₅, and TaCl₅ as catalysts, and *n*-Bu₄Sn as a cocatalyst. The polymerization reactions were carried out in toluene at either 30 or 80 °C. Monomer **M1** belongs to a mono-substituted acetylene. Both mixtures of WCl₆/*n*-Bu₄Sn and MoCl₅/*n*-Bu₄Sn are known to be active catalysts for the metathesis polymerization of mono-substituted acetylenes. In our study, the polymerization results of both catalyst mixtures are slightly different. A higher yield and number-average molecular weight were achieved for **PFA1** by using the WCl₆/*n*-Bu₄Sn as catalysts. The results demonstrate that **M1** can be polymerized even though it contains a bulky fluorene side group. Our results were agreed with many previous reports,^{29–31} which showed that the mono-substituted acetylenes can be polymerized without steric effect.

Monomers **M2–M5** belong to disubstituted acetylenes. According to the reports,^{32,33} the TaCl₅/*n*-Bu₄Sn mixture is known to be an active catalyst for the polymerization of sterically hindered diarylacetylene derivatives. Both monomers **M2** and **M3**, which contain an alkyl and a fluorenyl substituents, were polymerized by TaCl₅/*n*-Bu₄Sn in toluene at 80 °C for 24 h, yielding **PFA2** and **PFA3** with M_n of ~8 KDa in ~30% yield. Besides, **M4** and **M5**, which contain a phenyl and

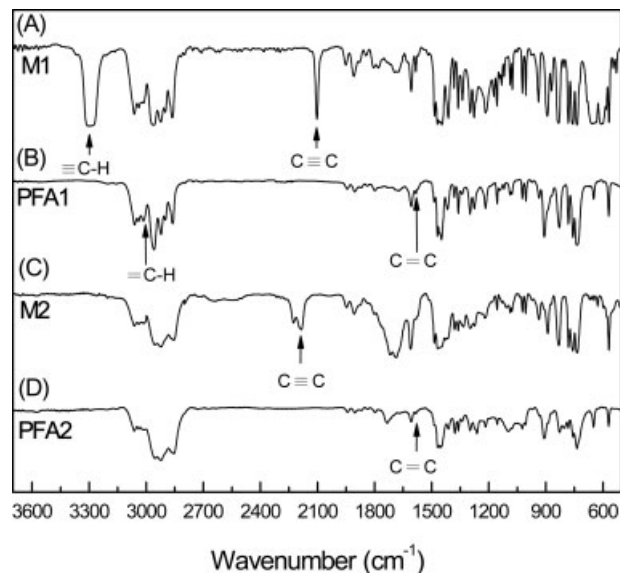


Figure 1. IR spectra for (a) **M1**, (b) **PFA1**, (c) **M2**, and (d) **PFA2**.

a fluorenyl substituents, were polymerized by $\text{TaCl}_5/n\text{-Bu}_4\text{Sn}$ in the same conditions, giving **PFA4** and **PFA5** with M_n of ~ 300 KDa in satisfactory yields ($\sim 70\%$). Comparing the polymerization results for **PFA2**–**PFA5**, we observed that the alkyl side group would hinder the metathesis polymerization of disubstituted acetylenes to produce **PFA2** and **PFA3** with lower molecular weights and yields.

Structure Characterization

Figure 1(b,d) shows the IR spectra of polymers **PFA1** and **PFA2**, respectively; for comparison, the spectra of their corresponding monomers **M1**

and **M2** [Fig. 1(a,c)] are also given. The monomer **M1** absorbs at 2130, 3293, and 630 cm^{-1} , due to the $\text{C}\equiv\text{C}$ stretching, $\equiv\text{C}-\text{H}$ stretching, and bending vibrations, respectively. All these acetylene absorption bands disappear in the spectrum of **PFA1**, but the double-bond $=\text{C}-\text{H}$ stretching at 3010 cm^{-1} appears, indicating that the acetylene triple bonds have been transformed to the polyene double bonds by the polymerization reaction. The monomer **M2** absorbs at 2226 and 2185 cm^{-1} , due to the $\text{C}\equiv\text{C}$ stretching, which disappear in the spectrum of **PFA2**. Instead, the double bond $\text{C}=\text{C}$ stretching at 1650 cm^{-1} appears. It has been reported by Simonescu and Percec that the *cis*- and *trans*- PPA can be determined by the $\text{C}=\text{C}-\text{H}$ out of plane and in plane deformation vibrations. The bands at 740, 895, and 1380 cm^{-1} are specific for *cis*-PPA, and the bands at 922, 970, and 1265 cm^{-1} are specific for *trans*-PPA. Comparing the spectra of **M1** and **PFA1**, most of the absorption bands in the figure-print region are very similar. Therefore, it is difficult to identify the *cis*- and *trans*- contents of **PFA1** by IR spectra.

The NMR analysis offers more detailed information on the molecular structure of the polymers. As shown in Figure 2(b), in the ^1H NMR spectrum of **PFA1**, there are no peaks in the absorption region of the acetylene protons ($\delta \sim 3.1$ ppm). Instead, a broad peak appears in the olefin and aromatic protons absorption region ($\delta \sim 6.8\text{--}8.0$ ppm). It has been reported by Simonescu and Percec that *trans*-olefin proton peak appears at 6.85 ppm and *cis*-olefin proton peak appears at 5.82 ppm. We can conclude that **PFA1**

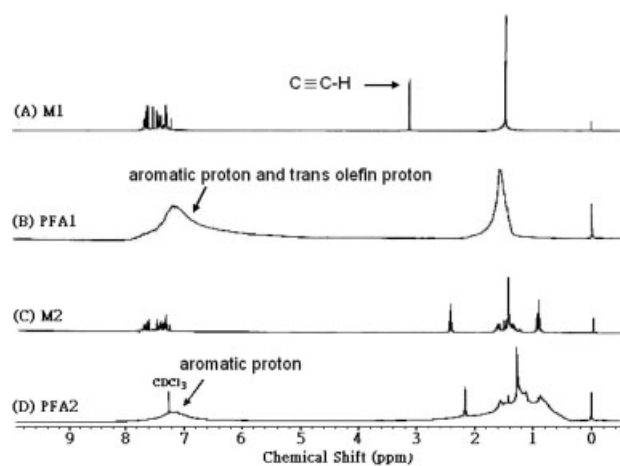


Figure 2. ^1H NMR spectra for (a) **M1**, (b) **PFA1**, (c) **M2**, and (d) **PFA2**.

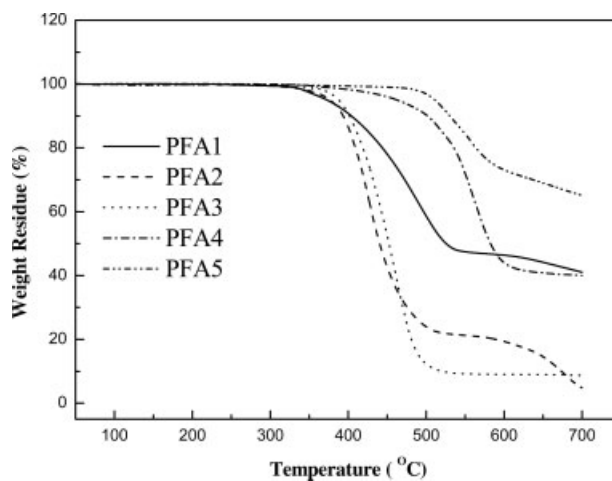


Figure 3. TGA thermograms of fluorene-containing polyacetylenes **PFA1**–**PFA5**.

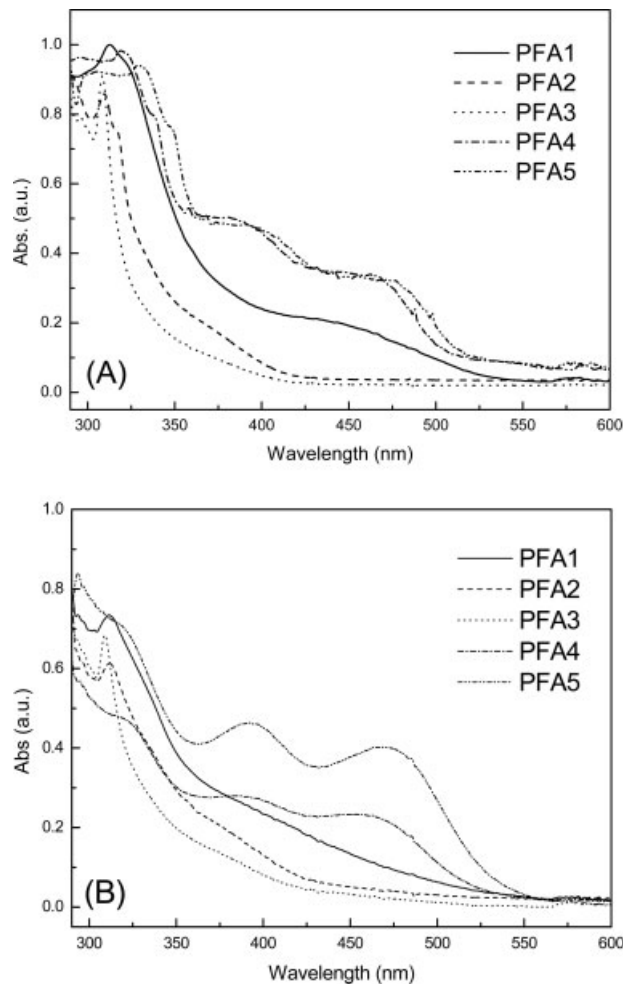


Figure 4. UV-vis absorption spectra of **PFA1–PFA5**. (a) in chloroform and (b) in thin film state.

synthesized by WCl_6 catalyst is a 100% trans structure. Since **PFA2–PFA5** belong to disubstituted polyacetylenes, they contain no olefinic protons. Therefore, it is impossible to identify their geometric isomers by ^1H NMR spectra.

The thermal properties of fluorene-containing polyacetylenes (**PFAs**) were investigated by TGA and DSC and summarized in Table 1. Figure 3 depicts the TGA traces of the polymers. **PFAs** show good thermal stability and their thermal degradation temperatures (T_d s) at 5% weight loss range from 370 to 503 °C. **PFA1** shows the lowest T_d at 371 °C and **PFA5** reveals the highest T_d at 503 °C. The glass-transition temperatures (T_g) are in the range from 76 to 84 °C. Again, the diaryl-substituted **PFA4** and **PFA5** exhibit higher T_g values. Furthermore, the polymers are soluble in common organic solvents, such as THF, chloroform, toluene, and xylene.

Optical Properties

Figure 4(a,b) depict the UV-vis absorption spectra of **PFA1–PFA5** in chloroform and in thin film state. For each polymer, both absorption spectra in the solution and in thin film state are very similar except for some peaks, which show a little redshift in the thin film state. This is reasonable since more chain aggregation occurs in the solid state. Comparing the five spectra of **PFA1–PFA5** in the thin film state, all polymers display an absorption peak near 310 nm, which is associated with the absorption peak of the fluorenyl side groups²⁶ and one or two broad absorption bands in the 350–550 nm region, which is attributed to the π - π^* interband transition of the main chains.³⁴

Figure 5(a,b) exhibit the PL spectra of **PFA1–PFA5** in chloroform and in thin film state. **PFA1** with a monofluorenyl substituent shows a maxi-

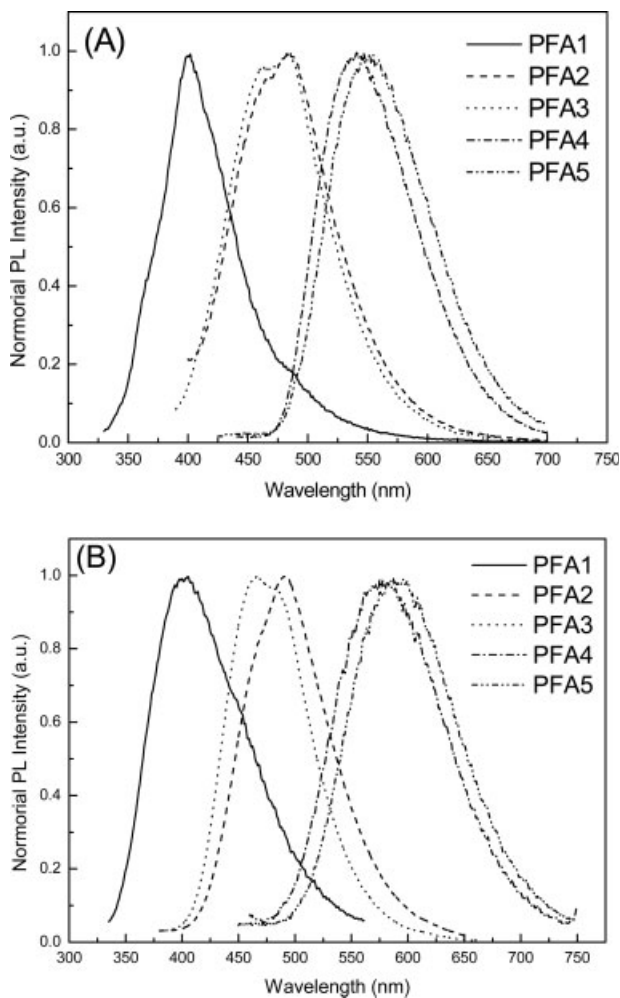


Figure 5. PL spectra of **PFA1–PFA5**. (a) in chloroform and (b) in thin film state.

Table 2. Optical Properties, Quantum Yields, and Redox Properties of PFA Polymers

Polymer	λ_{\max} (nm)				PL Efficiency ^e (solution, %)	Band Gap ^f (eV)	Eox (V)	HOMO/LUMO ^g (eV)
	Solution ^a		Film ^b					
	abs ^c	PL ^d	abs ^c	PL ^{c,d}				
PFA1	313	402	311	402	8	2.32	0.64	5.04/2.72
PFA2	312	483	312	486 (482)	79	2.95	0.7	5.10/2.15
PFA3	310	483	310	486	85	2.95	0.69	5.09/2.14
PFA4	320 (382,465)	541	388,459	546	50	2.44	0.86	5.26/2.82
PFA5	330 (391,476)	552	392,470	580	42	2.38	0.72	5.12/2.74

^a Measured in chloroform.^b Prepared by spin-coating from toluene solution.^c Data in the parentheses are wavelength of shoulders.^d Excited at λ_{\max} of abs.^e Measured by integral sphere in chloroform.^f The optical band gap takes as the absorption onset of UV-vis spectrum of the polymer film.^g HOMO/LUMO values as determined by the onset of CV measurements and optical band gap.

lum emission at 402 nm in chloroform. Its PL quantum efficiency (ψ_f) in chloroform is only 0.08. Theoretically, low luminescent efficiency is the result of solitons generation of the trans-structure of **PFA1**. Soliton formation is experimentally verified in an iodine-doped **PFA1**, causing to a new peak in the absorption spectrum. The result agrees with the PPA reported by Sun et al.¹¹ **PFA2** and **PFA3** belong to alkyl- and fluorenyl-substituted polyacetylenes, and emit a blue-green light at 483 nm in chloroform. Both ψ_f values of **PFA2** and **PFA3** are 0.79 and 0.85. **PFA4** and **PFA5** contain the phenyl- and fluorenyl-substituents in the polyacetylene main chains, and emit a green to yellowish green light at 541 and 552 nm in chloroform. Both ψ_f values are 0.50 and 0.42, respectively. These values are smaller than those of **PFA2** and **PFA3**. This could be due to more interchain quenching in the **PFA4** and **PFA5** system. Table 2 summarizes the UV-vis absorption and PL properties of **PFA1–PFA5**.

Electrochemical Properties

Cyclic voltammetry (CV) was employed to evaluate the ionization potential (i.e. hole-injection ability) and the redox stability of our **PFA**s. The oxidation and reduction potentials were used to determine the highest occupied (HOMO) and lowest unoccupied (LUMO) molecular orbital energy levels, which were calculated using the internal standard value of -4.4 eV with respect to the vacuum level. The anodic sweeps of **PFA**s (Fig. 6) were reversible and the oxidation onsets

occurred at potentials of $+0.64$ to $+0.72$ V for **PFA1–PFA5**. These oxidation potentials give HOMO energy levels ranging from -5.04 to -5.26 eV for **PFA1–PFA5**. The cathodic wave was not observed in acetonitrile solution for all of the polymers within solvent limit. However, the energy band gaps of **PFA**s can be estimated by the absorption onsets of their UV spectra. Using this approach, the calculated band gaps of **PFA1–PFA5** are in the range from 2.32 to 2.95 eV. The LUMO energy levels of **PFA1–PFA5** can be also estimated from optical band gaps and HOMO energy levels. The HOMO and LUMO energies levels of **PFA1–PFA5** are listed in Table 2, and the band diagrams of **PFA**s are shown in Figure 7. In this paper, the effects of substituents on the energy band gaps of the substituted polyacetylenes are investigated. Basically, there are two substitution related effects, electronic effect, and steric hindrance. Comparing the energy band gap of **PFA1** with those of the other disubstituted polyacetylenes, **PFA1s** shows a much smaller energy band gap. This is because **PFA1** has less steric effect and has longer conjugation length for the polyene main chains. In **PFA2** and **PFA4** case, **PFA2** contains alkyl and fluorenyl substituents, while **PFA4** contains phenyl and fluorenyl substituents. **PFA2** shows a much larger energy band gap than **PFA4**. This is because the alkyl substituent has larger steric effect than the phenyl substituent. In the case of **PFA4** and **PFA5**, the difference between two polymers is on the difluoro substituents. **PFA5** with a 2,3-difluorophenyl substituent exhibits a smaller energy

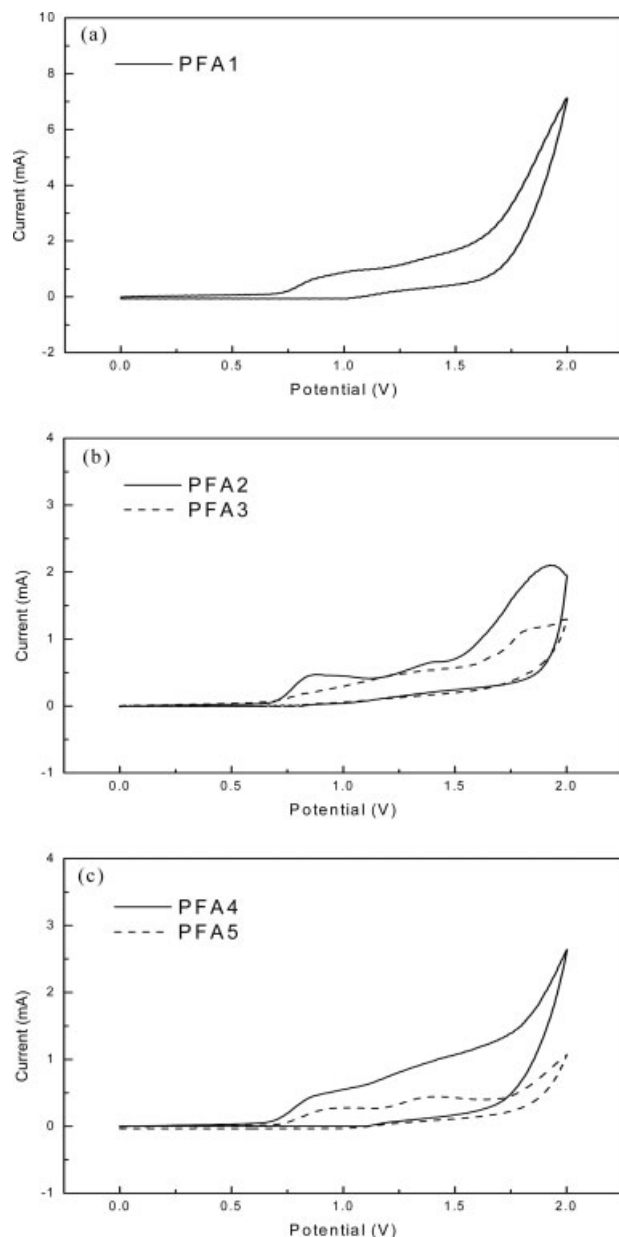


Figure 6. Cyclic voltammograms of **PFA1-PFA5** films.

band gap. This is due to the less electron withdrawing effect for the 2,3-difluorophenyl substituent than that of a phenyl substituent. The results are consistent with those reported by Sun et al.¹⁴

EL Properties and LED Devices

To evaluate the potential application of **PFA**s in PLED, we fabricated a double-layered device with the configuration of ITO/PEDOT/**PFA**s/Ca/Al. The EL spectra (Fig. 8) of the **PFA**s are simi-

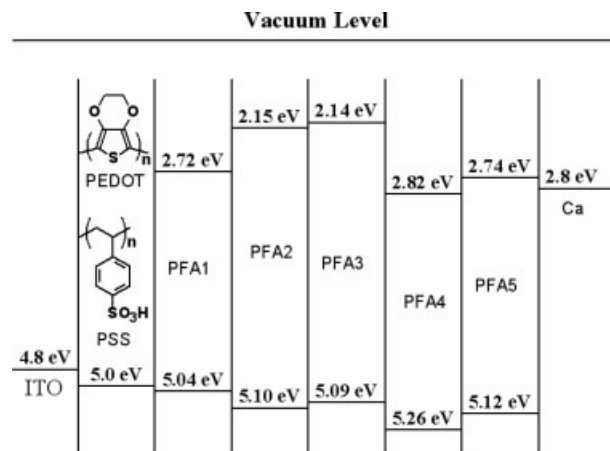


Figure 7. Energy level diagrams of **PFA1-PFA5**.

lar to their corresponding PL spectra (Fig. 4). This indicates that both the PL and EL spectra originate from the same radiative decay process of single excitons. Both **PFA2** and **PFA3** emit a blue light with peaks at 472 and 468 nm, respectively, while **PFA4** and **PFA5** emit an orange-red light with peaks at 576 and 602 nm, respectively. Besides, we don't observe the aggregate emission at a long wavelength, compared with the PL and EL spectra of polyfluorenes.²³ This means that the **PFA**s are more stable emitting materials than polyfluorenes.

Figure 9 exhibits the current density-luminance-voltage (I-L-V) plots for the devices fabricated with an emitting layer of **PFA2** and **PFA3**. The turn-on voltage of a **PFA2** device is 6 V, with a maximum brightness of 100 cd/m² at 14.5 V, whereas the turn-on voltage of a **PFA3** device is 6.3 V, with a maximum brightness of 77 cd/m² at 15 V. Both devices have much better performance

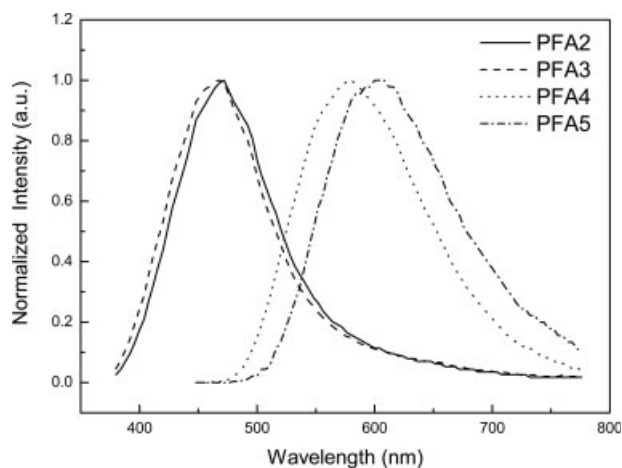


Figure 8. EL spectra of **PFA2-PFA5**.

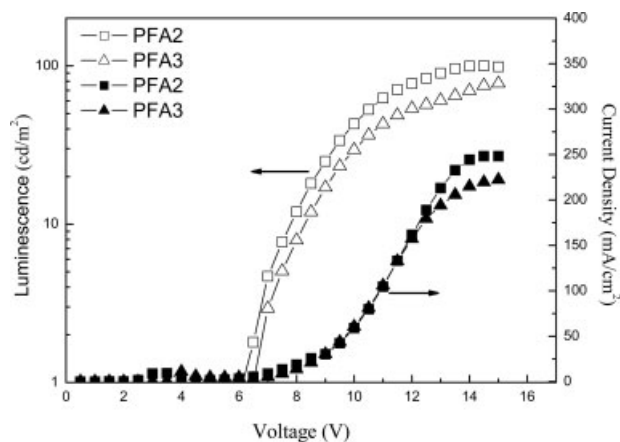


Figure 9. Current density and luminescence intensity-voltage characteristics for PFA2 and PFA3 in ITO/PEDOT/Polymer **PFA2** or **PFA3**/Ca/Al device.

than the blue devices based on poly(1-alkyl-2-phenylacetylene) reported in the literature.¹² This is because introducing the fluorene groups into the polyacetylene backbones would improve the charge injection of polymers, since **PFA**s show higher HOMO energy levels than poly(1-alkyl-2-phenylacetylene).

Figure 10 depicts the I-L-V characteristics of the PLED devices fabricated with **PFA4** and **PFA5**. The turn-on voltage of a **PFA4** device is 4.5 V, with a maximum brightness of 111 cd/m^2 at 8.5 V, while the turn-on voltage of a **PFA5** device is 2.8 V, with a maximum brightness of 923 cd/m^2 at 8 V. The **PFA5** device performance is the best for the red light devices based on polyacetylenes so far reported in the literatures.^{14,18}

Furthermore, it has been proven that a white PLED can be achieved by blending a blue host

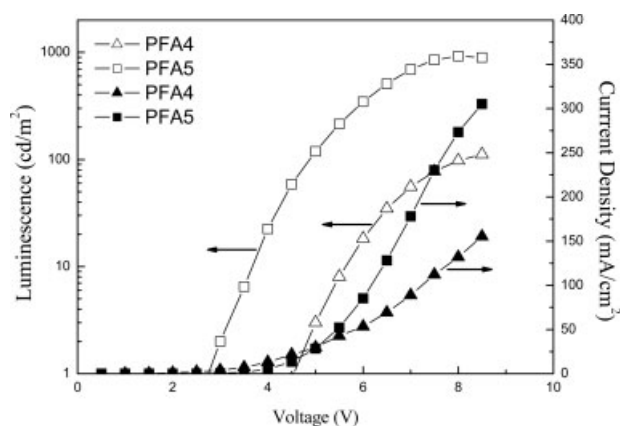


Figure 10. Current density and luminescence intensity-voltage characteristics for PFA4 and PFA5 in ITO/PEDOT/Polymer **PFA4** or **PFA5**/Ca/Al device.

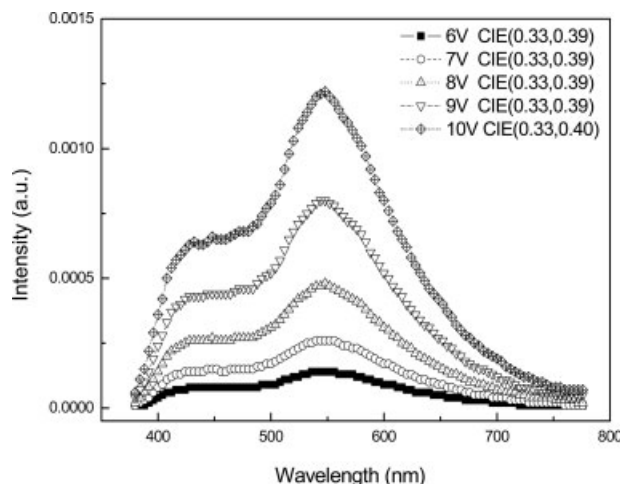


Figure 11. EL spectra measured at different voltage for the device: ITO/PEDOT/**PFA2** (98 wt %) + **PFA5** (2 wt %)/Ca/Al device.

polymer and an orange-red guest polymer.³⁵ We used **PFA2** as a host material, which was blended with 2 wt % of **PFA5** to yield a white light device. Figure 11 shows the EL spectra of the blended device. The EL intensity is increased as the voltage increases. However, no obvious color change is observed when the voltage increases. The CIE device coordinates ranges (0.33, 0.39) from 6 to 10 V. This demonstrates that **PFA**s are thermally stable when they are used as emitting layers in PLED. The I-L-V characteristics of blended polymers are shown in Figure 12. The turn-on voltage of this device is 6.0 V with a maximum current efficiency of 1.4 cd/A and a maximum brightness of 450 cd/m^2 at 15 V. This is a first highly efficient white light PLED device

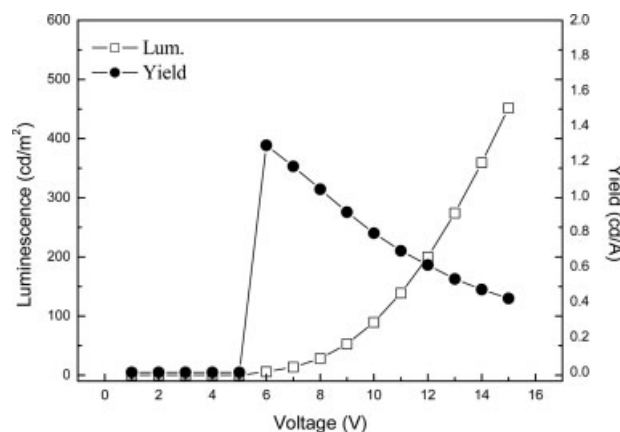


Figure 12. Luminescence and yield-voltage characteristics for the white light device: ITO/PEDOT/**PFA2** (98%) + **PFA5** (2%)/Ca/Al device.

Table 3. The EL Device Performances for PFA2–PFA5

Polymer	EL Emission λ_{\max} (nm) ^a	CIE Coordinate (x,y) ^a	Turn-on Voltage (V) ^b	Max Current Efficiency (cd/A)	Max Brightness cd/m ²
PFA2	472	(0.18,0.24)	6.0	0.03	100
PFA3	468	(0.17,0.18)	6.3	0.06	77
PFA4	576	(0.49,0.50)	4.5	0.07	111
PFA5	604	(0.54,0.45)	2.8	0.44	923
PFA2 (98 wt %) + PFA5 (2 wt %)	460,560	(0.33,0.39)	6.0	1.40	450

^a Recorded at 20 mA/cm².^b Recorded at 1 cd/m².

based on polyacetylenes. Table 3 summarizes the performances of the EL devices for the **PFA**s.

CONCLUSIONS

Five novel polyacetylenes containing fluorene side groups were successfully synthesized and characterized. The fluorene-substituted acetylene monomers can be polymerized by using $WCl_6/n-Bu_4Sn$, $MoCl_5/n-Bu_4Sn$, and $TaCl_5/n-Bu_4Sn$ as catalysts. Most of the **PFA**s were obtained in high molecular weights and reasonable yields. The monofluorenyl-substituted polyacetylene **PFA1** shows a maximum emission at 402 nm. Its PL efficiency in chloroform is only 0.08. Its EL property is too weak to be measured. However, **PFA2–PFA5** belong to disubstituted polyacetylenes. The bulky alkyl, phenyl, and fluorenyl groups were introduced to increase the steric hindrance and prevent close packing of the main chains. Both **PFA2** and **PFA3** emit blue-green light at 483 nm, while **PFA4** and **PFA5** emit a green to yellowish-green light at 541 and 552 nm in solution, respectively.

According to the CV results, the HOMO energy levels of **PFA2–PFA5** are located from 5.04 to 5.24 eV, which are higher than those of the disubstituted polyacetylenes reported in the literatures.³⁶ It means that the hole injection from ITO anode is much easier. This is the reason why **PFA2–PFA5** show much higher EL efficiency than the other disubstituted polyacetylenes. A device fabricated by **PFA5**, with the configuration of ITO/PEDOT:PSS/**PFA5**/Ca/Al, revealed a turn-on voltage at 2.8 V and a maximum brightness of 923 cd/m² at 8 V. This is the highest value for polyacetylenes reported in the literature so far. Furthermore, a white light PLED device based on the blending of 98 wt % of **PFA2**

and 2 wt % **PFA5** was also fabricated. The device shows a maximum current efficiency of 1.3 cd/A at 6 V and a maximum luminance of 450 cd/m² at 15 V. All these results demonstrate that disubstituted polyacetylenes are potential candidates for PLED applications.

The authors are grateful to the National Science Council of the Republic of China (NSC 93-2216-E-009-011) for its financial support of this work.

REFERENCES AND NOTES

- Burroughes, J. H.; Bradley, D. D. C.; Brown, A. R.; Marks, R. N.; Mackay, K.; Friend, R. H.; Burns, P. L.; Holmes, A. B. *Nature* 1990, 347, 539.
- Gustafsson, G.; Gao, Y.; Treacy, G. M.; Klavetter, F.; Colaneri, N.; Hegger, A. *J. Nature* 1992, 357, 477.
- Katz, H. E. *J Mater Chem* 1997, 7, 369.
- Marder, S. R.; Kippelen, B.; Jen, A. K. Y.; Peyghambarian, N. *Nature* 1997, 388, 845.
- Skotheim, T. A.; Elsenbaumer, R. L.; Reynolds, J. R. *Handbook of Conducting Polymers*, 2nd ed.; Marcel Dekker: New York, 1998.
- Hirakawa, S.; Musuda, T.; Takeda, K. In *The Chemistry of Tripolebonded Functional Groups*; Patai, S., Ed.; Wiley: New York, 1994.
- Simionescu, C. I.; Percec, V. *J Polym Sci Polym Chem Ed* 1980, 18, 277.
- Percec, V.; Rinaldi, P. L. *Polym Bull* 1983, 9, 548.
- Simionescu, C. I.; Percec, V.; Dumitrescu, S. *J Polym Sci Polym Chem Ed* 1977, 12, 2497.
- Percec, V. *Polym Bull* 1983, 10, 1.
- Sun, R.; Masuda, T.; Kobayashi, T. *Jpn J Appl Phys* 1996, 35, L1434.
- Sun, R.; Masuda, T.; Kobayashi, T. *Jpn J Appl Phys* 1996, 35, L1673.
- Nanjo, K.; Karim Abdul, S. A.; Nomura, R.; Wada, T.; Sasabe, H.; Masuda, T. *J Polym Sci Part A: Polym Chem* 1999, 37, 277.
- Sun, R.; Zheng, Q.; Zhang, X.; Masuda, T.; Kobayashi, T. *Jpn J Appl Phys* 1999, 38, 2017.

15. Sanda, F.; Nakai, T.; Kobayashi, N.; Masuda, T. *Macromolecules* 2004, 37, 2703.
16. Lee, P. P.; Geng, Y.; Kwok, H. S.; Tang, B. Z. *Thin Solid Films* 2000, 363, 149.
17. Xie, Z.; Lam, J. W. Y.; Dong, Y.; Qiu, C.; Kwok, H.; Tang, B. Z. *Opt Mater* 2002, 21, 231.
18. Chen, J. C.; Xie, Z.; Lam, J. W. Y.; Law, C. C. W.; Tang, B. Z. *Macromolecules* 2003, 36, 1108.
19. Lam, J. W. Y.; Tang, B. Z. *J Polym Sci Part A: Polym Chem* 2003, 41, 2607.
20. Ting, C. H.; Hsu, C. S. *Jpn J Appl Phys* 2001, 40, 5342.
21. Fujii, A.; Hidayat, R.; Sonoda, T.; Fujisawa, T.; Ozaki, M.; Vardeny, Z. V.; Teraguchi, M.; Masuda, T.; Yoshino, K. *Synth Met* 2001, 116, 95.
22. Leclerc, M. *J Polym Sci Part A: Polym Chem* 2001, 39, 2867.
23. Scherf, U.; List, E. J. W. *Adv Mater (Weinheim, Ger)* 2002, 14, 477.
24. Liu, B.; Yu, W. L.; Lai, Y. H.; Huang, W. *Chem Mater* 2001, 13, 1984.
25. Zhang, X.; Hogen-Esch, T. E. *Macromolecules* 2000, 33, 9176.
26. Mastroilli, P.; Nobile, F. C.; Crisorio, R.; Rizzuti, A.; Suranna, P. G.; Acierno, A. E.; Iannelli, P. *Macromolecules* 2004, 37, 4488.
27. Lee, S. H.; Jang, B. B.; Tsutsoi, T. *Macromolecules* 2002, 35, 1356.
28. Sohn, B. H.; Kim, K.; Choi, D. S.; Kim, Y. K.; Jeoung, S. C.; Jin, J. I. *Macromolecules* 2002, 35, 2876.
29. Abdul Karim, S. M.; Nomua, R.; Kajii, H.; Hidayat, R.; Yoshino, K.; Masuda, T. *J Polym Sci Part A: Polym Chem* 2000, 38, 4717.
30. Rivera, E.; Belletête, M.; Zhu, X. X.; Durocher, G.; Giasson, R. *Polymer* 2002, 43, 5059.
31. Kwak, G.; Masuda, T. *Polymer* 2002, 43, 665.
32. Masuda, T.; Takahashi, T.; Higashimura, T. *Macromolecules* 1985, 18, 311.
33. Teraguchi, M.; Masuda, T. *J Polym Sci Part A: Polym Chem* 1999, 37, 4546.
34. Patil, A. O.; Heeger, A. J.; Wudl, F. *Chem Rev* 1988, 88, 183.
35. Su, H. J.; Wu, F. I.; Shu, C. F. *Macromolecules* 2004, 37, 7197.
36. Hidayat, R.; Hirohata, M.; Fuji, A.; Teraguchi, M.; Masuda, T.; Yoshino, K. *Jpn J Appl Phys* 1999, 38, 931.